

## Phase transition and phonon characteristics of PbTiO<sub>3</sub> single-crystal nanorods prepared in NaCl flux

Cheng-ping Zhang<sup>1,2,3</sup>, Zhi-qiang Chen<sup>3,\*</sup> and Yu Deng<sup>1,2,\*</sup>

<sup>1</sup> Modern Analysis Center, Nanjing University, Nanjing 210093, China

<sup>2</sup> Physics School, Nanjing University, Nanjing 210093, China

<sup>3</sup> Center for High Pressure Science and Technology Advanced Research, Shanghai 201203, China

HPSTAR  
326-2016

**Keywords:** Phase transition, Phonon, TEM, Raman, Nanorod.

**Abstract.** By annealing PbTiO<sub>3</sub> (PT) nanoparticles together with surfactants in NaCl flux, single-crystal PT nanorods were prepared with diameters of 60–80nm and lengths of several micrometers. The PT nanorods are in tetragonal phase and grow along the (100) direction. A first-order phase transition from tetragonal ( $a=3.922\text{\AA}$  and  $c=3.963\text{\AA}$ ) to cubic ( $a=c=3.942\text{\AA}$ ) has been detected at 440°C. With the increasing temperatures from 25°C to 440°C, the Raman mode E(1TO) exhibits a soften behavior from  $74\text{cm}^{-1}$  to  $50\text{cm}^{-1}$ , whereas the mode B1+E keeps its frequency almost unchanged at  $286\text{cm}^{-1}$ . It is also noticed that both frequency and damping constant of mode E(1TO) show rapid changing with temperature only when temperature beyond 380 °C, below the temperature they change very gradually. To explain the particular properties of the PT nanorods, the formation mechanism and an enhanced size effect have been discussed.

### Introduction

Recently, the interests on one-dimensional nanostructures (1DNS) of perovskite oxides are continuously increasing due to their collective properties and novel applications [1-5]. Variety of techniques, such as solution-phase decomposition [1, 3], hydrothermal [5, 6], flux [2], template [4, 7], microemulsion [8] and electro-spinning [9] methods, have been developed to synthesize them. And many further researches are directed towards the detailed experimental investigations on their size-dependent properties [3, 4, 6, 10]. As an important perovskite oxide of excellent ferroelectric and optoelectronic characters, PT has been studied theoretically and experimentally in the past decades. Among these pioneer works, many efforts were focused on the size effect of PT nanocrystals and thin films [11-14]. The phase transition driven by the soft mode E(1TO) and the mode soften behaviors have been extensively investigated, proving that the Raman scattering is a very sensitive and effective method for size effect related researches [11-19]. Subsequently, series of theoretical and empirical equations have been established to describe the detailed relationships between their size and characters [11, 13, 15-17]. Now, referring to the 1DNS of PT, it's believed that the size and shape related properties should be more complex and attractive. In the communication, single-crystal PT nanorods were prepared by flux method and undertook a series of examinations with special attention to their phase transition and phonon properties. Our main aim is to give useful experimental results for better understanding of the particular size-dependent characters of PT nanostructures.

### Experimental

PT nanorods were synthesized by annealing fine PT nanocrystals together with surfactant nonylphenol ether (NP-9) in NaCl flux. The superfine PT nanoparticles were prepared by a modified sol-gel method [19], with an average size of 6.8nm. Then, the PT nanoparticles, NP-9 and NaCl were mixed by molar ratio of 1:5:20. The mixture was ultrasonic treated for 30 min, ground for 45 min, and then annealed at 700°C for 5 hours in air. The products were washed by distilled water for several times and then dried at 100°C. To ensure high purity of the products, all the reagents we used are of analysis pure level. X-ray diffraction (XRD) measurement was carried out on a Rigaku D/MAX-RA diffractometer with CuK $\alpha$  as an incident radiation. The morphology, microstructure and selected area

electron diffraction (SAED) of the samples were observed on a transmission electron microscope (TEM) of JEM-2100. Energy dispersive spectroscopy (EDS) was also performed. Raman scattering measurements were measured on a HR-800 Raman spectrometer under backscattering geometry, using 488nm exciting light at a power of 10mW. The thermal properties of the samples were examined on a PYRIS-1 differential scanning calorimeter (DSC). The Fourier transformation infrared spectra (FTIR) and the inductively coupled plasma resonance spectra (ICP) were detected on the instruments of NEXUS870 and J-A1100, respectively.

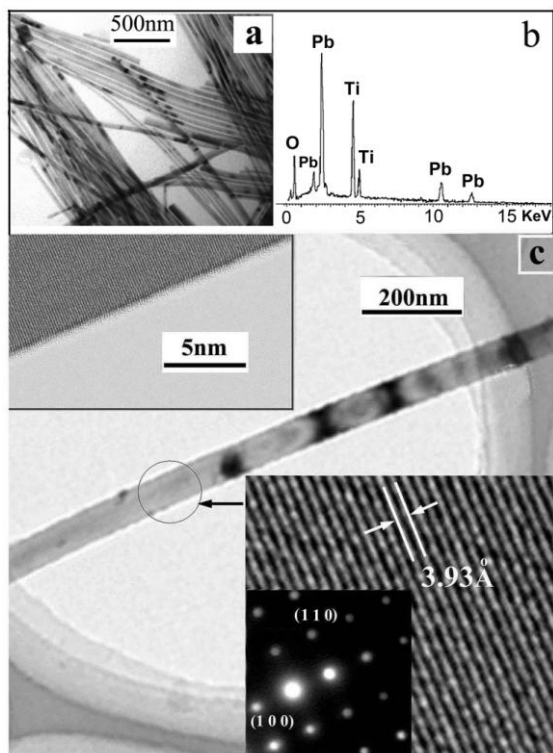


Figure 1. (a) TEM image of the PT nanorods; (b) EDS pattern of the PT nanorods; (c) TEM image of an individual PT nanorod with the upper inset for HRTEM image of its margin and the lower inset for HRTEM image of its 2D lattice fringes and the corresponding SAED pattern.

## Results and discussion

From the TEM image in Figure 1a, we can clearly see that the as-prepared PT nanorods were uniform and well isolated, with diameter of 60-80 nm and length of several micrometers. Notably, though some nanorods prolong in length, they exhibit almost the same diameter widths. Fig. 1b depicts the EDS pattern of the samples. Within the instrumental accuracy, it's revealed that the PT nanorods are pure with a stoichiometric proportion of Pb:Ti = 1:1. The result was then confirmed by ICP spectroscopy examination, demonstrating that the ratio of Pb:Ti was 1.00:1.01. HRTEM observation was performed at the center region of an individual PT nanorod and illustrated in Fig. 1c. As the HRTEM image shown in the upper inset of Fig. 1c, the margin of the nanorod is smooth and well crystallized, without dislocations or layer faults. The lower inset of Fig. 1c represents the two-dimensional (2D) lattice fringes and the corresponding SAED pattern, indicating the PT nanorod is in tetragonal phase [11, 20]. The inter-planar spacing is measured to be 3.93Å, corresponding to the lattice constant  $a$ , which implies that the nanorod should grow along (100) direction.

Figure 2 plots the XRD patterns of the PT nanorods under various temperatures. The diffraction lines at room temperature (25°C) can be perfectly indexed as the tetragonal-phase PT [11, 20]. The lattice constants of  $a$  and  $c$  are calculated to be 3.922Å and 3.963Å, respectively. It is in good agreement with above HRTEM measurements. Comparing with bulk crystal ( $a_{crystal} = 3.899Å$ ,  $c_{crystal}$

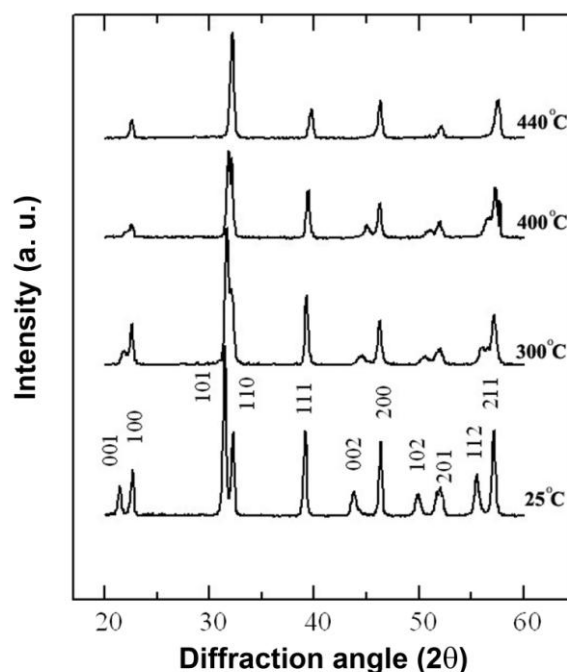


Figure 2. The XRD patterns of the PT nanorods under various temperatures.

= 4.153Å), the *a*-elongation and *c*-shortening of the nanorod lead to a notable decrease of the tetragonality *c/a*. As a result, the cell of the PT nanorods shows a volume shrinking (60.959Å<sup>3</sup>) than PT bulk crystal (63.135Å<sup>3</sup>). We suggest that the shrinking of cell volume in the nanorods should be related to the surface tension and size effect, which is similar to the cases in PT nanocrystals and thin films [11, 13]. When temperature increased, the shifting of diffraction line (101) to higher and (110) to lower angle are observed. Gradually, this two diffraction lines get more and more close until finally overlapped at 440°C, declaring that the PT nanorods transform from tetragonal into cubic structure. During the transition process with increasing temperatures, the similar phenomenon also take place between the diffractions lines of (001) and (100), (002) and (200), (102) and (201), (112) and (211), respectively. Fig. 3 shows the variation of lattice constants *a* and *c*, together with the tetragonality *c/a* of the PT nanorods, as functions of the temperatures. When temperature increased from 25°C to 440 °C, the lattice constant *a* increased from 3.922 Å to 3.942Å, and *c* decreases from 3.963 Å to 3.942 Å, leading to the decreasing of the *c/a* which almost approaches 1.00 at the transition temperature. It should be noticed that the cell volume of the cubic-phase PT nanorod is smaller than cubic-phase PT crystal [19, 21], which can be also attributed to the size effect [11]. In the upper inset of Fig.3, the DSC curve of the nanorods is depicted. A typical heat flow peak can be observed at a transition-zone between 428°C to 460°C, indicating that the phase-transition is a first-order one [19, 20, 22].

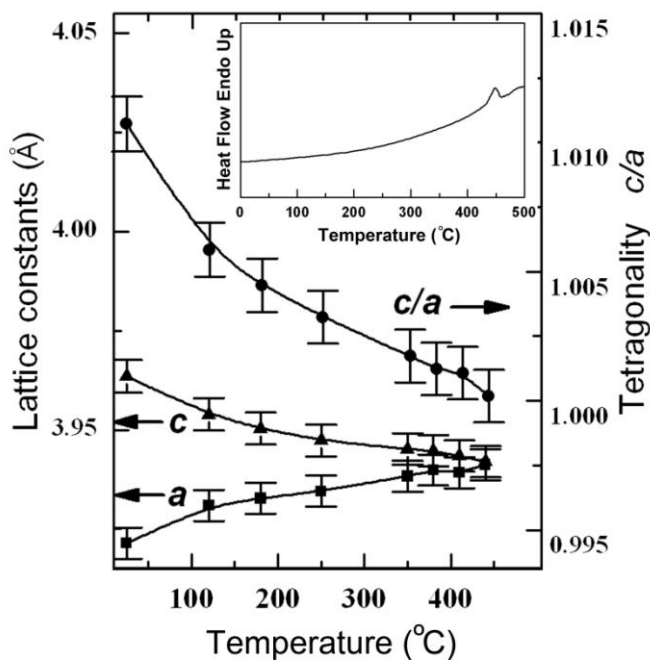


Figure 3. The lattice constants *a*, *c* and the tetragonality *c/a* of the PT nanorods under different temperatures, with the upper inset for the DSC curve of the PT nanorods.

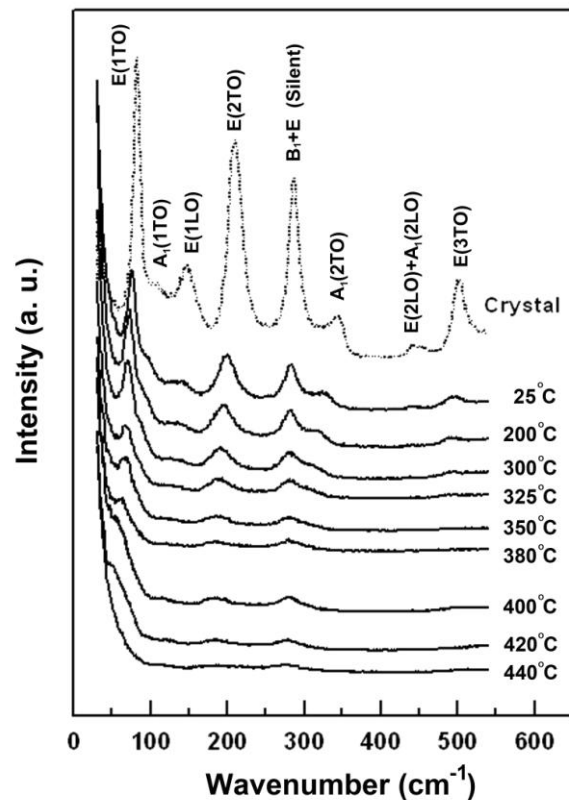


Figure 4. Raman spectra of the PT nanorods at different temperatures, in comparison to the spectrum of PT bulk crystal at room temperature (dash line).

In Figure 4, the solid-line curves depict the Raman spectra of PT nanorods at various temperatures. All modes of the Raman lines have been successful assigned and compared to the PT crystal spectrum (dash-line curve in Fig. 4) [11, 18]. Comparing with crystal, all the Raman lines of nanorods at room temperature represent notable decreasing in intensity and broadening in line-width. Except the mode B<sub>1</sub>+E, which located at 286cm<sup>-1</sup> and almost the same as crystal value, all Raman modes of the nanorods have lower frequencies than crystal. When temperature rising from 25°C to 440°C, we can see that the “silent mode” B<sub>1</sub>+E [18, 20] firmly keeps its frequency without

downshifting like other modes, though its Raman line also shows weakening and broadening. The stiffening of the mode  $B_{1+E}$  can reflect the rigidity of the oxygen octahedral in the lattice of PT nanorods [11, 18, 20, 23], ensuring that there is little distortion happened to the octahedral structure. Earlier investigations on doped PT have discovered that the impurities can also cause the decreasing of tetragonality, accompanying with broadening and weakening of Raman lines [12, 14]. However, in the doped PT the frequency shifting of  $B_{1+E}$  was distinctly observed, since the impurities change the valence state of oxygen [12, 14, 24, 25]. As known, for PT the size effect does not affect the frequency of  $B_{1+E}$  [11, 18]. Considering there are few impurities or defects in the nanorods, the steadfastness of mode  $B_{1+E}$  in PT nanorods can be well explained. As shown in Fig.4, the lowest-frequency Raman line of the nanorods is indexed as the “soft mode”  $E(1TO)$ , which locates at  $74\text{ cm}^{-1}$  for room temperature,  $8\text{ cm}^{-1}$  downshifting than crystal [18, 23]. It’s known that the softening of mode  $E(1TO)$  drives a ferroelectric-to-paraelectric (tetragonal-to-cubic) phase transition [11, 18, 23]. With increasing temperature, we can see that the  $E(1TO)$  line keep downshifting and weakening until it disappears at the frequency of  $50\text{ cm}^{-1}$  when temperature reaches  $440^{\circ}\text{C}$ . Well consistent with above XRD data,  $440^{\circ}\text{C}$  is therefore regarded as the transition point of the PT nanorods. The PT nanorods exhibits not only a notable transition-point dropping ( $53^{\circ}\text{C}$  lower than crystal), but also a notable weakened softening behavior of the  $E(1TO)$  mode ( $13\text{ cm}^{-1}$  downshift from  $74\text{ cm}^{-1}$  to  $51\text{ cm}^{-1}$ ) than PT crystal ( $31\text{ cm}^{-1}$  downshift from  $82\text{ cm}^{-1}$  to  $51\text{ cm}^{-1}$ ) [11]. The reduction of tetragonality in the PT nanorods should be responsible for it, which also leads to weakening of ferroelectricity [11, 12, 18, 23]. Fig. 5 depicts the frequency and the damping constant of  $E(1TO)$  mode as the functions of temperatures, where the damping constant dominates the shape of the Raman peak [11, 18, 23]. With increasing temperature, the mode frequency downshifts and damping constant increases. Noticeably, for both frequency and damping constant of  $E(1TO)$ , we can see that they change gradually below  $380^{\circ}\text{C}$ , and following with an abrupt changing beyond this temperature. The weak soften behaviors and the large damping constant suggest that the lattice vibration of the PT nanorods is evidently softer than PT crystal [11, 12, 18, 23], which is similar to the case of PT nanoparticles and should mainly originate from the size effect [11].

We know for these PT nanorods with diameters of 60-80nm, the fraction of surface layers is relatively small. Interestingly, they exhibit a rather large size effect in comparison to PT nanocrystals and thin films with same ratio of surface layers [11-14]. To understand it, the growth mechanism was investigated and the intermediate steps of the synthesizing process were traced. From Figure 6a, the TEM image of the intermediate products which were annealed at  $700^{\circ}\text{C}$  for 30 min, we can see that some rod-like 1DNS have already emerged. Further observation by HRTEM (upper left inset in Fig. 6a) reveals that the 1DNS is actually agglomerated nanoparticles enveloped by surfactants. The PT nanorods seem to crystallize from these self-organized nanoparticles under the aids of surfactants [7, 26]. The supposal is confirmed by the TEM and HRTEM images in Figure 6b, where the 1DNS are found to crystallize into nanorods after being annealed for 1 hour. However, it is noticed that the nanorods are short and they can keep growing by further annealing. We also find that both length and diameter of the nanorods are independence on cooling-speed. In addition, by FTIR investigations on the intermediate products, it is revealed that the surfactants do volatilize gradually instead of burning out soon in the annealing process. These evidences strongly imply that the “annealing growth” mechanisms as Ostwald ripening [27, 28] are more suitable for our PT nanorods than the “cooling growth” mechanisms as VLS theory [29]. Thus, we suggest that formation of nanorods should be attributed to three parts of modified assembling, recrystallizing and oriented attaching growth, as the schematic diagram depicted in Fig 6c. Since the PT nanorods are formed by the point-initiated uniaxial crystal growth, the lattice of them will be rigidly arrested from expansion [26, 30, 31]. It should contribute to the size effect of the PT nanorods. More, the surface-limiting effect induced by surfactants can also influence the lattice and phase-transition properties of the PT nanorods. As known, in the synthesis process the surfactants can not only enhance the surface tension of the nanostructures but also work as “surfactant template”, which will also limit the lattice [2, 7, 11, 28]. The remarkable cell shrinking and tetragonality decreasing induced by size effect have also been

observed in the BaTiO<sub>3</sub> and SrTiO<sub>3</sub> nanostructures prepared through surfactant system [2, 7]. In contrast, the PT nanorod by surfactant-free method shows less change in lattice than crystal, though the size effect was observed as well [6]. Therefore, we suggest that the both the point-initiated growth kinetics of nanorods and the surfactants used in synthesis process contribute to the enhancing of the size effect. More detailed investigations on the size dependent ferroelectric and optoelectronic properties of the PT nanorod are being carried out in our group.

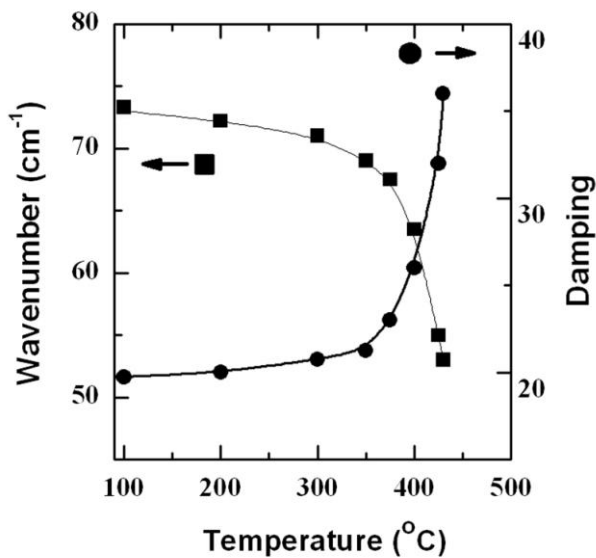


Figure 5. The frequencies and the damping constants of PT nanorods' E(1TO) mode at various temperatures.

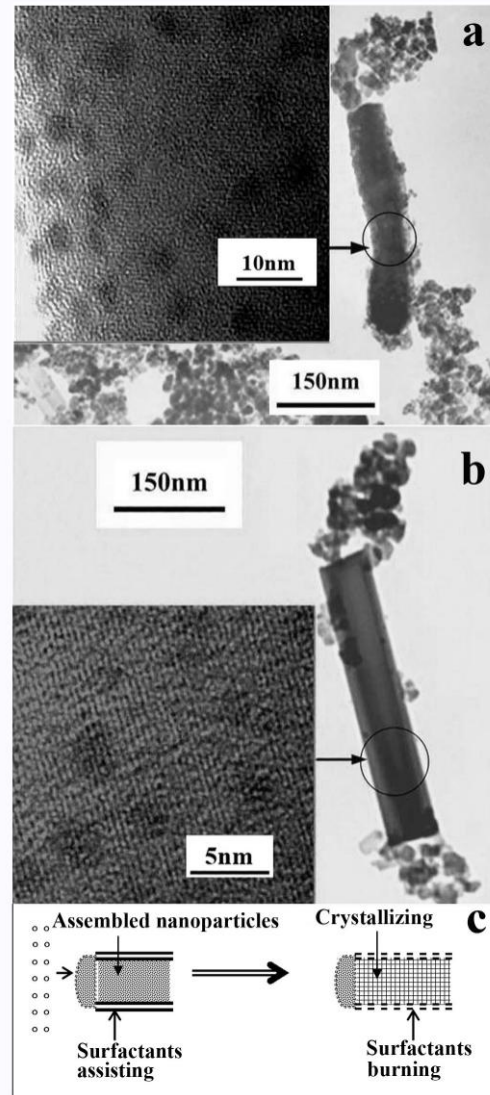


Fig. 6 (a) The TEM image of the intermediate product after annealing at 700°C for 30 min; (b) The TEM image of the intermediate product after annealing at 700°C for 1h with upper inset for its HRTEM image; (c) The supposed schematic diagram for the PT nanorods

## Summary

In summary, we studied the phase transition and phonon properties of single crystal PT nanorods prepared by annealing the PT nanoparticles with NP-9 in NaCl flux. The Curie point is determined by Raman scattering to be 440°C, which is 53°C lower than crystal. A weaker soften behavior of mode E(1TO) was revealed, implying a weaker ferroelectricity. In comparison to crystal, the decreasing of tetragonality and shrinking of cell have also been detected. The particular properties of the PT nanorods are attributed to an enhanced size effect. Further investigation on the formation mechanism of the nanorods suggest that the point-initiated growth of nanorods and the surfactants used in preparing process should be responsible for the enhancing of the size effect.

## Acknowledgement

The authors acknowledge the support of Natural Science Foundation of Jiangsu Province, China (Grant No. BK20151382) and NSAF (Grant No. U1530402).

## References

- [1] J. J. Urban, W. S. Yun, Q. Gu, H. Park, *J. Am. Chem. Soc.* 124, (2002) 1186.
- [2] Y. B. Mao, S. Banerjee, S. S. Wong, *J. Am. Chem. Soc.* 125 (2003) 15718.
- [3] J. J. Urban, J. E. Spanier, L. Ouyang, W. S. Yun, H. Park, *Adv. Mater.* , 15, (2003) 423.
- [4] X. Y. Zhang, X. Zhao, C. W. Lai, J. Wang, X. G. Tang, J. Y. Dai, *Appl. Phys. Lett.* 85, (2004) 4190.
- [5] G. Xu, Z. Ren, P. Du, W. Weng, G. Shen, G. Han, *Adv. Mater.* 17, (2005) 907.
- [6] H.S. Gu, Y. M. Hu, J. You, Z. L. Hu, Y. Yuan, T. J. Zhang, *J. Appl. Physic.* 101 (2007) 024319.
- [7] S. Y. Zhang, F. S. Jiang, G. Qu, C. Y. Lin, *Materials Letters*, (2008) 48.
- [8] W. P. Chen, Q. Zhu, *Materials Letters*, 61 (2007) 3378.
- [9] X. Lu, D. Zhang, Q. Zhao, C. Wang, W. Zhang, Y. Wei, *Macromol. Rapid Commun.*, 27 (2006) 76.
- [10] W. S. Yun, J. J. Urban, Q. Gu, H. Park, *Nano Lett.* 2 (2002) 447.
- [11] K. Ishikawa, K. Yoshikawa, N. Okada, *Phys. Rev.*, B 37 (1988) 5852.
- [12] Y. Deng, Z. Yin, Q. Chen, M.S. Zhang, W.F. Zhang, *Mater. & Sci. Eng.*, B 84 (2001) 248.
- [13] M. de Keijser, G. J. M. Dormans, P. J. van Veldhoven, D. M. de Leeuw, *Appl. Phys. Lett.* 59 (1991) 3556.
- [14] S. Yakovlev, C. H. Solterbeck, E. Skou, M. Essouni, *Appl. Phys. A* 82 (2006) 727.
- [15] I.P. Batra, P. Wurfel, B. D. Silverman, *Phys. Rev. Lett.* 30 (1973) 384.
- [16] I.P. Batra, P. Wurfel, B. D. Silverman, *Phys. Rev. B* 8 (1973) 3257.
- [17] Y. Umeno, T. Shimada, T. Kitamura, C. Elsasser, *Physical Review B* 74 (2006) 174111.
- [18] G. Burns, B. A. Scott, *Phys. Rev. Lett.* 25 (1970) 167.
- [19] Y. Deng, M. S. Zhang, J. L. Wang, Q. R. Gu, *Inter. J. Modern Phys. B* 19 (2005) 2669
- [20] Z. Tomeno, Y. Ishii, Y. Tsunoda, K. Oka, *Physical Review B* 73 (2006) 064116
- [21] O. Yamaguchi, A. Narai, T. Komatsu, K. Shimizu, *J. Am. Ceram. Soc.* 69 (1986) C-256.
- [22] R. J. Nelmes, W. F. Kuhs, *Solid State Comm.* 54 (1985) 721.
- [23] G. Burns, B. A. Scott, *Phys. Rev. B*, 7 (1973) 3088.
- [24] R. E. Cohen, *Nature* 358 (1992) 136.
- [25] Y. Kuroiwa, S. Aoyagi, A. Sawada, J. Harada, E. Nishibori, M. Takata, M. Sakata, *Physical Review Letters*, 87 (2001) 217601.
- [26] Z. Y. Tang, N. A. Kotov, M. Giersig, *Science* 297 ( 2002) 237.
- [27] P.W. Vorhees, *Annu. Rev. Mater. Sci.* 22 (1992) 197.
- [28] W. Wang, C. Xu, G. Wang, Y. Liu, C. Zheng, *Adv. Mater.* 14 (2002) 837.
- [29] S. Sharma, M.K. Sunkara, *Nanotechnology* 15 (2004) 130.
- [30] J. D. Holmes, K. P. Johnston, R. C. Doty, B. A. Korgel, *Science* 287 (2000) 1471.
- [31] H. L. Wang, X. D. Ma, X. F. Qian, J. Yin, Z. K. Zhu, *J. Solid State Chem.* 177 (2004) 4588.